JOURNAL OF GEOPHYSICAL RESEARCH, VOL. 108, NO. B2, 2076, doi:10.1029/2001JB000691, 2003

A method for measuring the solid particle permittivity or electrical conductivity of rocks, sediments, and granular materials

D. A. Robinson[1] and S. P. Friedman

Institute of Soil, Water, and Environmental Sciences, ARO, Volcani Center, Bet Dagan, Israel

Received 18 June 2001; revised 6 April 2002; accepted 31 May 2002; published 6 February 2003.

[1] Measurement of the effective dielectric permittivity of porous media provides an elegant method of estimating both the porosity and water content of soils, sediments, and rocks. Obtaining accurate estimates of water content can only be achieved if the models relating the measured permittivity to water content work well. One of the difficulties with testing physical models describing two- and three-phase dielectric mixtures (saturated and unsaturated systems) is obtaining an accurate value for the permittivity of the mineral matrix. No direct measurement method has been presented for rocks and soils, so the solid permittivity value is often an estimate of 5, essentially remaining a fitting parameter. We present a measurement method requiring no preassumed theoretical model. The method requires the measurement of the effective permittivity of a granular material immersed in fluids of differing permittivity and interpolation between the range of data points. Measurements of the permittivity of the mineral matrix of a number of materials are presented, including glass beads (7.6), quartz sand (4.7), calcareous seashell fragments (8.9), hematite ore (18.1), tuff (6.0), and a sandy loam soil (5.1). Estimates based on using mixing models to obtain the solid permittivity are demonstrated to underestimate the permittivity of hematite ore by between 0% and 45%, depending on the model and packing. The method is also suitable for measuring the electrical conductivity of granular minerals by changing the electrical conductivity of the bathing solution. Results for the electrical conductivity of hematite ore (0.040 dS m^{-1}) and carborundum (10.9 dS m^{-1}) are presented. *INDEX TERMS:* 1645 Global Change: Solid Earth; *KEYWORDS:* TDR, dielectric, solid, mineral, permittivity, mixing

Citation: Robinson, D. A., and S. P. Friedman, A method for measuring the solid particle permittivity or electrical conductivity of rocks, sediments, and granular materials, *J. Geophys. Res.*, *108*(B2), 2076, doi:10.1029/2001JB000691, 2003.

1. Introduction

[2] Measurement of the permittivity of the mineral matrix of a granular solid is of interest within geophysical, remote sensing and hydrological research. Within hydrology the measurement of the effective permittivity of soils, sediments and rocks is often used to estimate their water content [*Topp et al.*, 1980; *Sen et al.*, 1981; *Hallikainen et al.*, 1985; *Dirksen and Dasberg*, 1993; *Heimovarra et al.*, 1994; *Kraszewski*, 1996]. Direct calibration between measured permittivity and water content is not always possible, nor always desirable. Therefore, the use of dielectric mixing models to estimate water content from the measured permittivity of either saturated or unsaturated materials is often preferred [*Dobson et al.*, 1985; *Sihvola*, 1996; *Friedman*, 1998; *Chan and Knight*, 1999]. One of the difficulties with effectively testing models is that the permittivity of the mineral matrix is often unknown. The value for quartz in the literature is given as 4.3–4.7 [*Carmichael*, 1982] depending on crystal orientation and so values around this are often quoted for the permittivity of the mineral matrix.

[3] Tables giving values of the permittivity of solid minerals are often estimated from the effective permittivity of a repacked granular sample [*Olhoeft*, 1981; *Nelson*, 1992]. The standard method for obtaining solid permittivity values for geological minerals has been to use a mixing model to determine the permittivity of the solid from that of a granular mixture in air. This is unsatisfactory as it relies on assumptions in mixing models being correct, something we know not to be the case. The approach preassumes the correctness of the theoretical model. Achieving accurate estimates of solid permittivity using repacked granular materials is not trivial as the permittivity of a two-phase mixture depends on a number of factors. The relationship between the effective permittivity of a two-phase mixture and the bulk density to which it is packed is nonlinear. Complicating this further is the particle shape [*Jones and Friedman*, 2000] and particle size distribution [*Robinson and Friedman*, 2001], both of which affect the measured permittivity. Considerable efforts have been made to predict the solid permittivity (ε_s), using mixing models describing the effective permittivity (ε_{eff}) of

[1]Now at US Salinity Laboratory, USDA, Riverside, California, USA.

0148-0227/03/2001JB000691$09.00

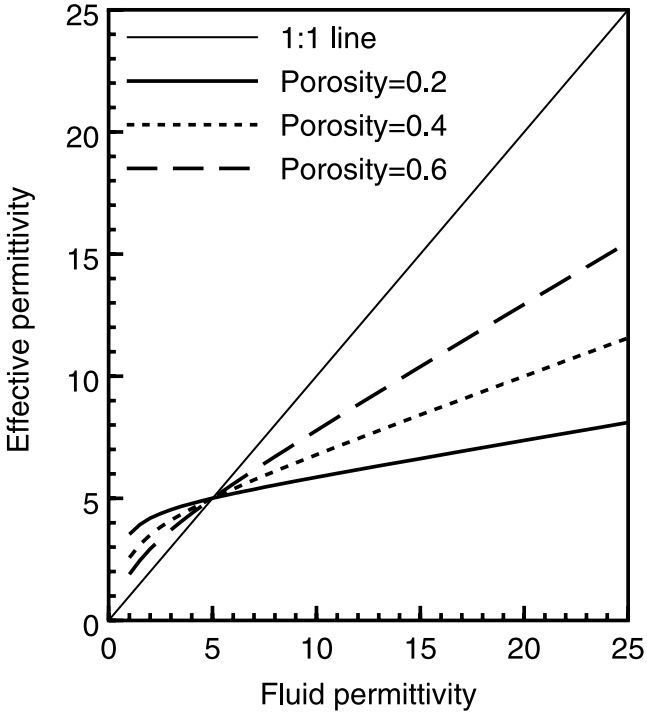

Figure 1. Effective permittivity as a function of the background permittivity modeled using the Maxwell Garnett formula (equation (3)). A solid with permittivity of 5 is modeled with three porosities to demonstrate the porosity independence of the crossing point between the effective permittivity and the 1:1 line.

a two-phase granular mixture, packed to different bulk densities in air. *Olhoeft* [1981] used the expression (1a) based on the *Lichtenecker* [1926] equation (1b), which simply averages the logarithms of the permittivities, this must be considered a power law approximation and lacks a rigorous theoretical base:

$$\varepsilon_s = \varepsilon_{eff}^{\frac{1}{1-\phi}} \tag{1a}$$

$$\ln \varepsilon_{eff} = \phi \ln \varepsilon_o + (1-\phi) \ln \varepsilon_s \tag{1b}$$

where ϕ is the porosity and ε_o, is the permittivity of the background. *Nelson et al.* [1989] favored the *Looyenga* [1965] mixing formula:

$$\varepsilon_s = \left[\frac{\varepsilon_{eff}^{1/3} + f - 1}{f}\right]^3 \tag{2a}$$

$$\varepsilon_{eff}^{1/3} = \phi\varepsilon_0^{1/3} + f\varepsilon_s^{1/3} \tag{2b}$$

where f, (1-ϕ) is the volumetric fraction of the solid inclusion. In subsequent work they found that equations (1a) and (1b) over predicted values of the solid permittivity for low permittivity plastics [*Nelson and You*, 1990]. The difficulty with this approach is that no rigorously tested dielectric mixing model for two-phase, randomly packed, granular material has been developed to date. *Dube* [1970] for example, tested the Looyenga model for powders pointing out that the error in predicting the solid permittivity could be as much as 8% for the mixtures studied in his work, however, the error can be much higher, as will be demonstrated further on. Estimates of the solid permittivity using this approach are thus limited by the quality of the models and assumptions therein. An independent measurement method of determining the permittivity of the solid in a granular material is therefore of some interest.

2. Theoretical Considerations

[4] The approach followed in this work was to propose a method for determining the matrix permittivity of a granular solid by immersing it in a range of dielectric fluids. The immersion of a granular material in a dielectric fluid gives an effective permittivity measured in the 0.1–1 GHz range somewhere between the permittivity of the background fluid ε_0, and the permittivity of the granular solid inclusions ε_s of volume fraction, f. This might not be the case at low frequencies where other polarization phenomena may contribute to the effective permittivity. By changing the permittivity of the immersion liquid the effective permittivity also changes. This is best illustrated using a dielectric mixing model to demonstrate the general trends. The choice of modeling approach is largely influenced by the wavelength at which measurements are conducted. Scattering effects are encountered if the wavelength is of a similar magnitude to the particle size. In our case the wavelength is much greater than the particle size and so it is safe to use effective medium theory. The *Maxwell-Garnett* [1904] mixing model based on the *Lord Rayleigh* [1892] formula

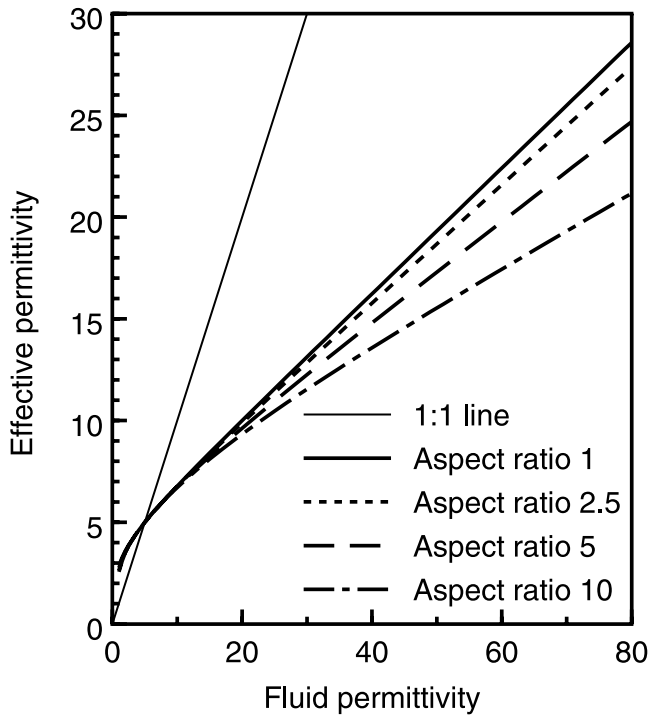

Figure 2. Effective permittivity as a function of the background permittivity modeled using a Maxwell Garnett type formula (equation (4)) for an isotropic random packing of oblate ellipsoids with increasing aspect ratio, (porosity = 0.4).

Table 1. Granular Materials and Physical Properties

Material	Particle Density, g cm^{-3}	Porosity	Predominant Mineralogy	Minor Constituents
Glass spheres 500 μm	2.49	0.395	Sodium silicate glass	
Quartz sand 500 μm	2.65	0.382	Quartz	
Sea shell fragments 6 mm	2.83	0.584	Calcite/Aragonite	
Hematite ore 1500 μm	4.13	0.508	Hematite 70%	Quartz 30%
Tuff 1500 μm	2.88	0.619	Volcanic glass 30%	Iron oxides 11%
			Amorphous minerals 20%	Halloysite 10%
				Others 29%
Sandy loam soil >500 μm	2.60	0.419	Quartz	Iron oxide
Carborundum 500 μm	3.17	0.458	Silicon carbide	

is the most commonly used model for describing a two-phase mixture and best suited to the present discussion:

$$\varepsilon_{eff} = \varepsilon_0 + 3f\varepsilon_0\left(\frac{\varepsilon_s - \varepsilon_0}{\varepsilon_s + 2\varepsilon_0 - f(\varepsilon_s - \varepsilon_0)}\right) \quad (3)$$

The model assumes that the solid spherical inclusions "see" around themselves only the permittivity of the background. In reality in a densely packed granular mixture the background seen by the solid is some combination of solid and fluid and its respective permittivity. This means that the Maxwell-Garnett model is expected to be an upper bound where the background has a higher permittivity than the inclusion and a lower bound when this is reversed. The error between measured and predicted effective permittivity is therefore expected to increase as the contrast ($\varepsilon_0/\varepsilon_s$) between the two phases increases.

[5] Figure 1 illustrates the relationship between the effective permittivity, ε_{eff}, and the fluid permittivity, ε_0, for a granular material with $\varepsilon_s = 5$, packed to three different porosities according to equation (3). The 1:1 line is plotted on the diagram and it can be seen that all the lines converge to the same point on the 1:1 line as the effective permittivity approaches the value of the fluid permittivity. The 1:1 line crossing point is physically significant, as this point is where the permittivity of the fluid is the same as the permittivity of the solid and the two-phase mixture appears as a single dielectric to the measuring device. Above this point the effective permittivity is reduced below the permittivity of the immersion fluid and below this point the effective permittivity is greater than that of the immersion fluid.

[6] Particle shape and orientation can strongly influence the effective permittivity [*Jones and Friedman*, 2000], especially as the contrast between the fluid and inclusion increases. The strength of the proposed method is that these effects do not influence the measurement of the solid permittivity, unlike the estimates obtained from repacked powders. Figure 2 illustrates this point using the Maxwell-Garnett type mixing formula for isotropic mixtures of oblate ellipsoidal particles [*Sihvola and Kong*, 1988; *Jones and Friedman*, 2000]:

$$\varepsilon_{eff} = \varepsilon_0 + \left\{\left[\sum_{i=a,b,c}\frac{f(\varepsilon_s - \varepsilon_0)\varepsilon_0}{3[\varepsilon_0 + N^i(\varepsilon_s - \varepsilon_0)]}\right] \cdot \left[1 - \sum_{i=a,b,c}\frac{fN^i(\varepsilon_s - \varepsilon_0)}{3[\varepsilon_0 + N^i(\varepsilon_s - \varepsilon_0)]}\right]^{-1}\right\} \quad (4)$$

where the terms are as previously described and the summation (i) is over the three principal axes of the ellipsoids. The depolarization factors (N^i) describing the extent to which the inclusion polarization is reduced according to its shape and orientation with respect to the applied electrical field are approximated by *Jones and Friedman* [2000]:

$$N^a = \frac{1}{1 + 1.6(a:b) + 0.4(a:b)^2} \quad N^b = 0.5(1 - N^a) \quad (5)$$

where a:b is the particle aspect ratio of an ellipsoid of revolution as defined by *Jones and Friedman* [2000], where, $N^a + N^b + N^c = 1$, and $N^b = N^c$. Thus, the depolarization

Table 2. Measured Permittivity Values of Fluids Used in the Experiments at 25°C

Fluid	Permittivity
Air	1.0
Penetrating oil	2.3
Methylene chloride	8.8
Acetone	20.8
Water	78.6

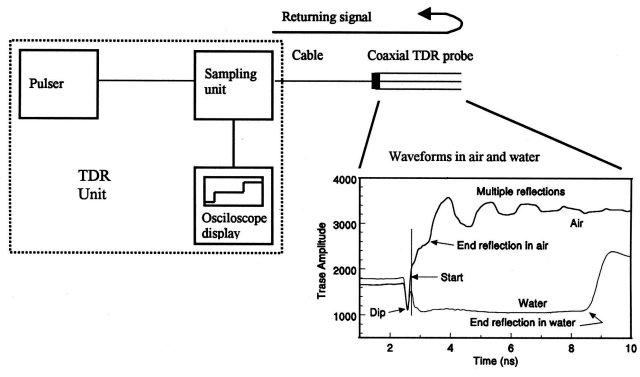

Figure 3. A schematic diagram of the experimental design, including the TDR and coaxial cell in which the measurements were made. Two waveforms are presented for air and water. The travel time from which the permittivity was measured is the time measured between the line marked start and the respective points marked end reflection.

Table 3. Estimated Values of Solid Permittivity From Measurements by Immersion in Dielectric Fluids[a]

Material	Measured Permittivity	Literature Estimate
Glass spheres 500 μm	7.6 (r^2 = 0.999)	6.75 (1)
Quartz sand 500 μm	4.7 (r^2 = 0.999)	4.3–4.7 (2)
Sea shell fragments 6000 μm	8.9 (r^2 = 0.999)	Calcite 8.3–8.6 (3)
Hematite ore 1500 μm	18.1 (r^2 = 0.999)	Hematite 25 (2) Hematite/quartz mix 18.9
Tuff 1500 μm	6.0 (r^2 = 0.999)	2.7–12.2 (4)
Sandy loam soil >500 μm	5.1 (r^2 = 0.995)	4.7 (2)

[a]Column two gives permittivity estimates from the following literature: (1) *Von Hippel* [1954]; (2) *Carmichael* [1982]; (3) *Lide* [1999]; and (4) *Olhoeft* [1981].

factors for a sphere are $N^{a,b,c}$ = 1/3, 1/3, 1/3. So long as the contrast between the background and inclusion phase is maintained below about 4, the ε_{eff} of the oblate ($a \leq b = c$) particles does not depend significantly on shape (Figure 2). Therefore, it appears justified to use the simpler equation (3) in the subsequent analysis where the dielectric contrast is less than 3. The alternative method uses an empirical best fit regression line fitted to the data, the permittivity of the solid is then calculated from its fit at the intersection point with the 1:1 line. This method is discussed first in the results section. The major concern is for the reproducibility of the packing, which can be reasonably achieved by maintaining a constant porosity.

3. Materials and Methods

3.1. Granular Media

[7] A range of natural dielectric materials was chosen from different environments to test the method. Spherical glass beads (Mo-Sci Corp., Rolla, MO, USA), made of soda lime silicate glass were chosen as a reference spherical material. All the materials are listed along with their properties in Table 1, the particle densities were determined using a standard excluded volume method.

3.2. Dielectric Immersion Fluids and Packing

[8] One of the difficulties in applying this type of method is finding fluids whose permittivities lie in a range between 1 and 15. The fluids must not exhibit relaxation at the frequency of measurement and they must have a viscosity that allows the granular material to be mixed in the fluid, low viscosity fluids being the best. Air and Acetone provide the limits of interest (Table 2), with methylene chloride (dichloromethane) and penetrating oil (WD-40®) mixtures covering the range of greatest interest. We found that alcohol is unsuitable as relaxation occurs in the MHz–GHz frequency range used here. Acetone and water, which are miscible, were used to cover the higher permittivity ranges.

[9] The granular samples were carefully packed into a coaxial waveguide to a known porosity in air for the first set of measurements. The sample was then reconstituted, the same volume fraction of solid was maintained for the subsequent measurements in other fluids to keep a constant porosity, given in Table 1.

3.3. Measurement of the Effective Permittivity

[10] The time domain reflectometry (TDR) method [*Topp et al.*, 1980; *Gardner et al.*, 2000] was used to measure the permittivity of the samples. The velocity of a plane electromagnetic wave is:

$$v = \frac{c}{\sqrt{\mu_r \varepsilon_r}} \tag{6}$$

where c is the velocity of light (3×10^8 ms^{-1}), μ_r is the magnetic permeability of the material and ε_r is the relative permittivity. TDR measures the propagation velocity of a step pulse that has a wide bandwidth, usually 10 kHz–3 GHz. The effective frequency measured by the TDR depends on the TDR probe design and the risetime of the TDR signal. In the case of the Tektronix TDR like the one used here the majority of the signal has been reported to lie between 50 MHz and 1000 MHz, with most of the energy being associated with the 300 MHz region [*Friel and Or*, 1998]. The magnetic permeability is unity in most Earth materials so the wave velocity is a function of just the permittivity of the medium through which it travels.

[11] Schematic diagrams of the TDR unit and a section of transmission line are presented in Figure 3. A step voltage is applied between the conductors in the TDR at the pulse generator. The signal propagates down the line and is reflected from the end of the probe, which is covered by the repacked sample; the returning signal is sampled in the TDR. The velocity of the signal is therefore:

$$v = \frac{l}{t} \quad \text{and} \quad v = \frac{c}{\sqrt{\varepsilon_r}} \tag{7}$$

where l is the length of the TDR probe in meters and t is the time in seconds. Equating these two and rearranging gives the round trip propagation time (t) of the wave as a function of both the length of transmission line (l) and the permittivity of the material surrounding it.

$$t = \frac{2l\sqrt{\varepsilon_r}}{c} \tag{8}$$

Hence it follows that the permittivity can be found by measuring the time it takes the wave to traverse the probe, if the one way travel time is used the 2 drops out of equation (8). Waveforms for air and water are presented in Figure 3 to

Table 4. Results of Repeated Measurements of Glass Beads Demonstrating the Precision Achieved Using the TDR Method

Fluid Composition	Measured Solution Permittivity	Effective Permittivity of Mixture	Measurement Standard Deviation
Air	1.0	3.7	0.1
Oil	2.7	5.0	0.2
Acetone/water mixture	27.9	14.0	0.1
Acetone/water mixture	58.3	22.8	0.1

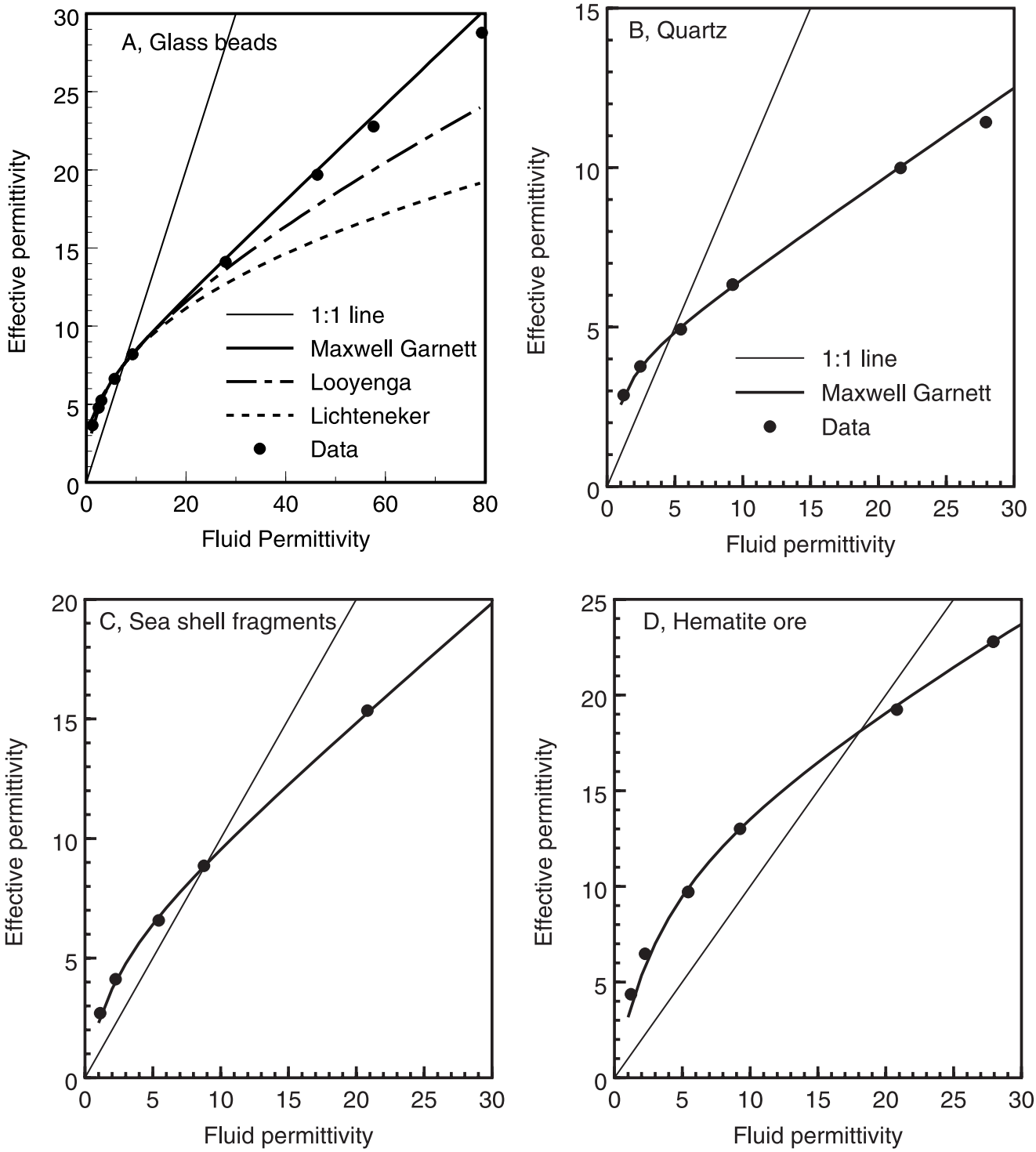

Figure 4. a–f. Measured effective permittivity of six granular materials as a function of the permittivity of the immersion fluid. 3a. Measurements obtained with glass beads are presented along with the Maxwell Garnett (equation (3)), Lichtenecker (equations (1a) and (1b)) and Looyenga (equations (2a) and (2b)) model fits using the respective determined solid permittivity values (Table 3).

demonstrate that the time is measured from the place marked "start" to the points marked "end reflection" and show that the time increases as the permittivity of the material increases.

[12] A Tektronix (1502C) time domain reflectometer (TDR) cable tester was used throughout the experiments to measure the effective permittivity. The TDR was connected to a PC, which was used to collect and analyze waveforms using software developed by *Heimovaara and de Water* [1993]. The software fits tangent lines to the waveform to locate the end reflection and uses this to calculate travel time from which permittivity is determined.

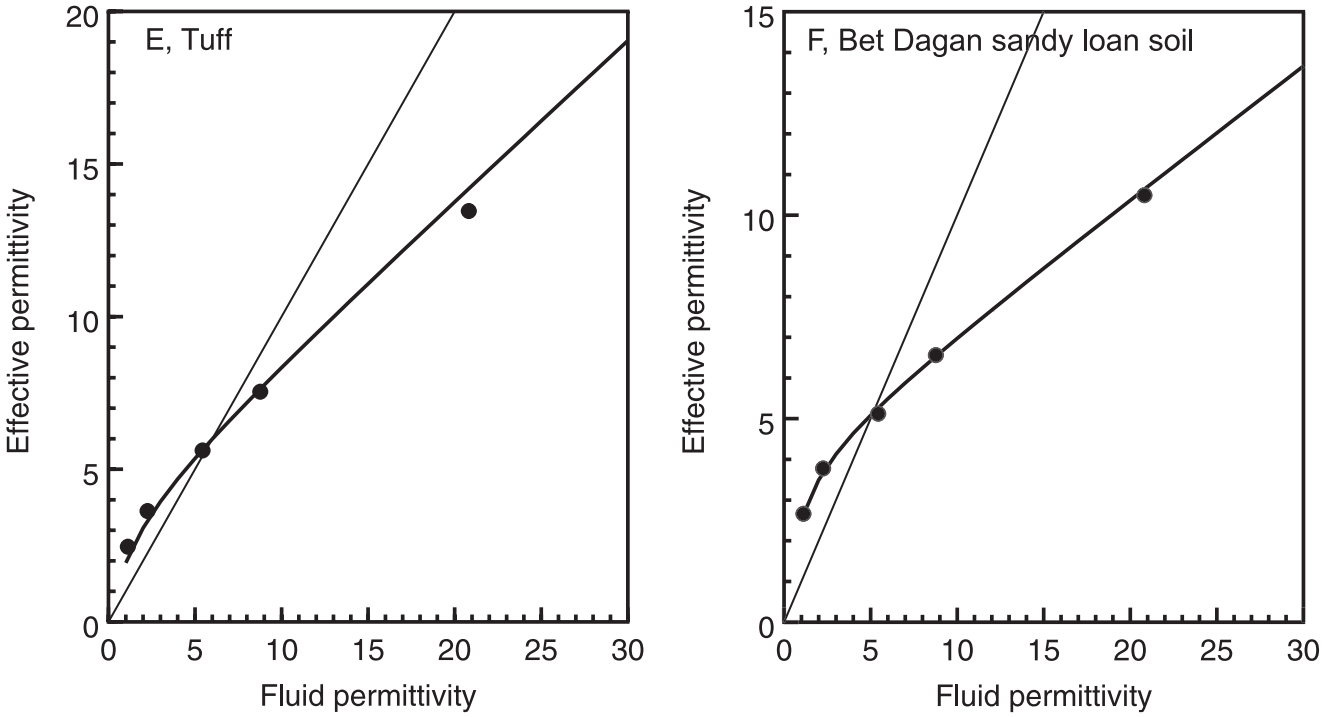

Figure 4. (continued)

The TDR was connected via a 1.8 m, (50-ohm RG 58) coaxial cable to a coaxial waveguide, constructed from steel, 200 mm long with an internal diameter of 26.5 mm and a 6 mm diameter inner electrode. The waveguide was calibrated for effective length using de-ionized water and air in a similar manner to *Heimovaara* [1993]. Ten waveforms were collected using the TDR device and averaged to measure the effective permittivity of the mixture.

3.4. Measurement of the Bulk Electrical Conductivity and Solid Electrical Conductivity

[13] Two-phase dielectric and electrical conductivity are considered analogous physical transport problems [*McKenzie and McPhedran*, 1977] at the scale of interest in this work. Therefore, the method outlined for determining the permittivity of solid grains should by analogy be suitable for determining the electrical conductivity of solid grains. Instead of using a dielectric as the background fluid an ionic solution of potassium chloride is used. The values of the ionic conductivity of this solution are varied in the range suitable for the material under test. Two granular materials, hematite and carbourundum (SiC) were used to test this approach, they were repacked in solutions with different electrical conductivity values, σ_w. Measurements of apparent electrical conductivity were made at a frequency of 1 kHz A.C. using a Radiometer CDM83 conductivity meter. This was attached to a small stainless steel coaxial cell 10 mm high with a 50 mm outer diameter and 10 mm inner diameter electrode.

4. Results and Discussion

4.1. Measured Dielectric Permittivity of Solid Grains

[14] Measurements were made using the six materials placed in at least five dielectric solutions. A power function of the form $\varepsilon_{eff} = a + b\varepsilon_0^c$ was found to give a good empirical fit to the data points. The obtained curve was then used to find the intersection with the 1:1 line by equating ε_{eff} with ε_0 and solving iteratively for ε_0 to determine, ε_s. The results are presented in Table 3 along with reported values from the literature. Estimates collected from the literature, though often similar, do not necessarily coincide with the measured values. The reasons for this can be the use of different measuring frequencies and different chemical compositions, but also erroneous determination methods relying on inadequate dielectric mixing models. The likely errors involved with measuring the permittivity with the method described are most likely to be involved with the accuracy with which one packs the electrode container and the accuracy of the device used to measure permittivity. In our experiments we used TDR to measure the effective permittivity. An example of the precision of the measurements obtained using glass beads is presented in Table 4., in general the precision is found to be ±0.1 permittivity units. Thus, the results presented for the solid permittivity should be accurate to within ±0.2 using the proposed methodology.

[15] The results for the glass beads are slightly higher than previously published [*Robinson and Friedman*, 2001]; quartz sand falls within the expected range. The seashells have a higher permittivity than measurements made on pure calcite; this is most likely due to aragonite in the seashells, which has a higher permittivity than calcite. The value for hematite ore is similar to the predicted value considering that the exact hematite/quartz ratio was not known. Values obtained from the literature for the permittivity of tuff are of too broad a range to provide meaningful comparison, however, our sample does fall within the range. The permittivity of the soil is slightly higher than the value for quartz, which is considered to be due to the iron oxide coatings on the quartz grains.

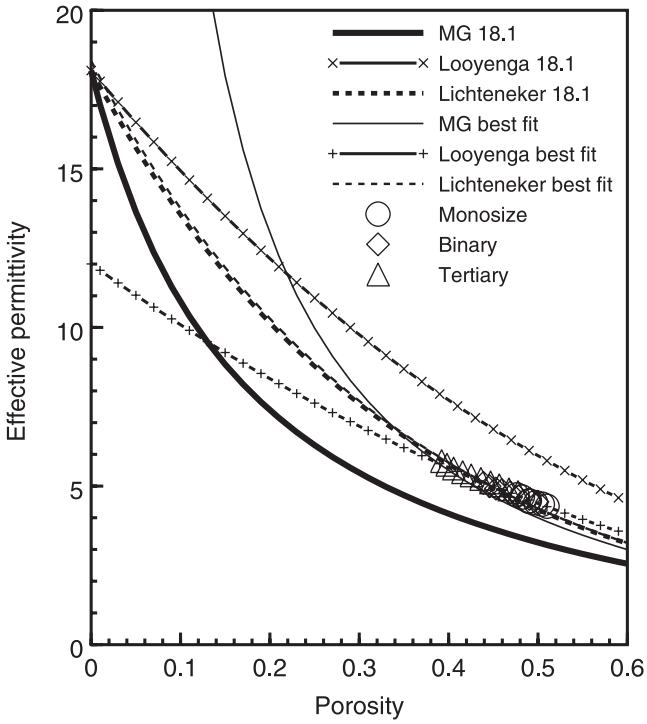

Figure 5. The effective permittivity of hematite ore in air for a range of porosities. The Lichtenecker (equations (1a) and (1b)), Looyenga (equations (2a) and (2b)) and Maxwell Garnett (equation (3)) models are presented in the first instance using the empirically determined permittivity value of the solid (lines 1, 2 and 3 in the legend) and Second with the best fit to the data (lines 4, 5 and 6 in the legend). Size fractions: 0.85 mm monosize, 0.85 (50%) and 0.50 (50%) mm binary and 0.85 (33.3%), 0.5 (33.3%) and <0.18 (33.3%) mm tertiary.

[16] The ε_{eff} (ε_o) results used for the determination of the solid permittivity of the six materials are presented in Figure 4. The Maxwell-Garnett (equation (3)), Looyenga (equation (2b)) and Lichteneker (equation (1b)) model predictions are compared with the glass bead data in Figure 4a, using the determined solid permittivity value of 7.6 (Table 3). The Maxwell-Garnett model is considered the most physically rigorous formula and lies closest to the data. The Maxwell-Garnett model is an exact solution to the Laplace equation and is strictly applicable to dilute mixtures. In lattice structures [*McKenzie and McPhedran*, 1977] where particles are in contact the Maxwell-Garnett solution becomes an upper bound and permittivity values are expected to fall slightly below it. This is observed as the dielectric contrast ($\varepsilon_o/\varepsilon_s \cong 10$) increases as expected. The other models are more limited physical descriptions and their inadequate predictive ability is clearly demonstrated with the data.

[17] Figures 4b–4f present the Maxwell-Garnett predictions with the data and not the empirical power functions actually used for the determination of the ε_s values listed in Table 3. The Maxwell-Garnett predictions (equation (3)) correspond well with the data, even though the granules were not spheres. This is because the contrast range is small enough to reduce the effects of grain shape to being negligible. It suggests that the use of the model fitted to 2 or 3 relevant data points could reduce the effort required to determine the permittivity of the solid. This will depend on the level of accuracy required to determine the solid permittivity.

5. Comparison of Immersion Measurement With Mixing Model Predictions of the Solid Permittivity

[18] The difficulty with determining the permittivity of the solid using mixing models is illustrated in Figure 5. This presents measurements made with mixtures of differing size fractions of hematite ore, packed in air to achieve a broad range of porosity. Predictions based on the Lichtenecker, Looyenga and Maxwell-Garnett models (equations (1b), (2b), and (3) respectively) are presented, using the value of 18.1 determined for the solid permittivity. Lines representing the best-modeled fit with the data by adjusting the permittivity of the solid are also presented. The Lichtenecker model gives a good fit to the data but this must be considered coincidental as the poor predictive value of the model was demonstrated in Figure 4a. The predictions of the solid permittivity obtained by best fitting the models to all the data were; 18.4 using the physically poor Lichtenecker model, the erroneous prediction of 12 for the Looyenga model and an adjustment to an infinite value of ε_s still did not allow a fit between the data and the Maxwell-Garnett model. As the Maxwell-Garnett model is considered to be the most physically rigorous model the lack of fit with the data suggests the

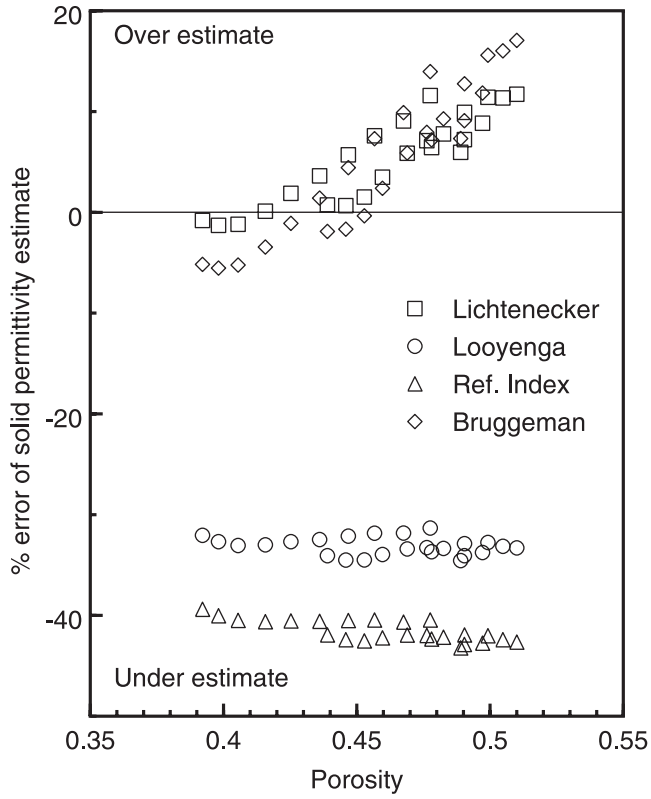

Figure 6. The % error between the determined solid permittivity according to the proposed immersion method (ε_s = 18.1) and the predicted permittivity using equations (1a), (2a), (6), and (7) with measurements in air.

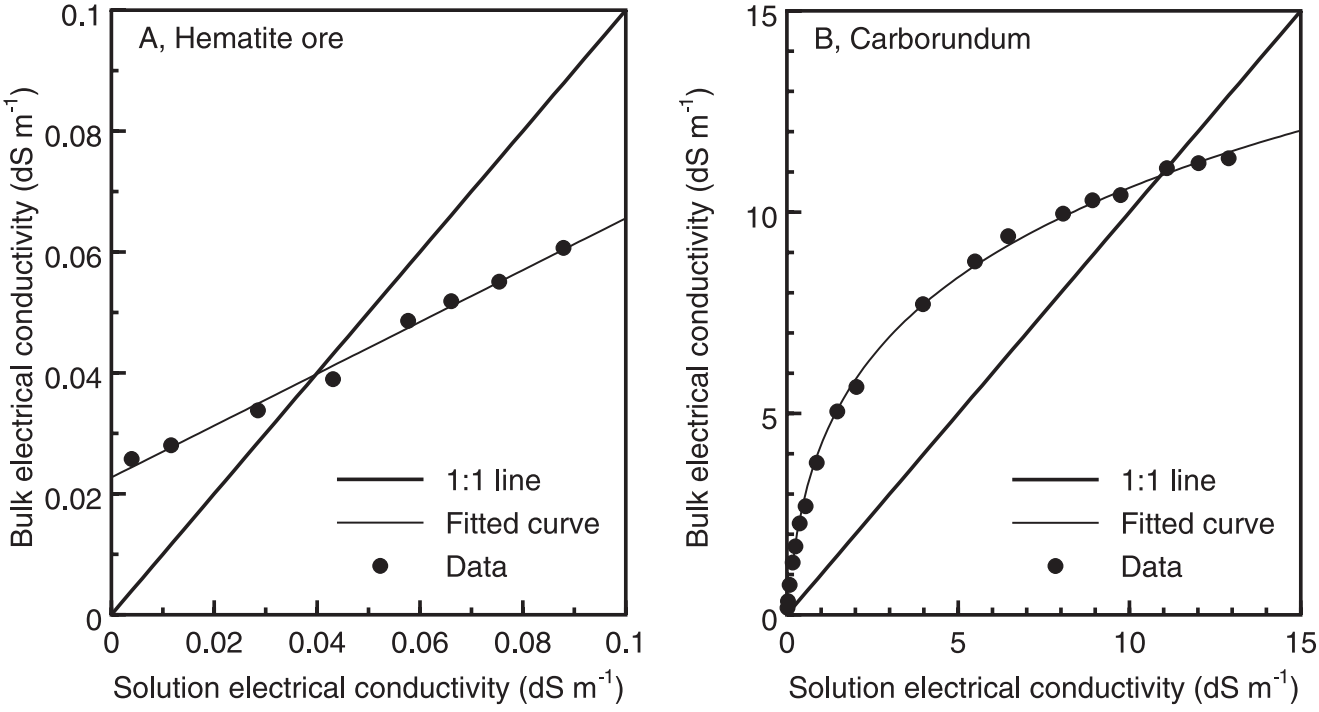

Figure 7. The apparent bulk electrical conductivity of semiconducting grains in KCl solutions of increasing electrical conductivity. The intersection point between the fitted curve and the 1:1 line is used to determine the electrical conductivity of the solid.

importance of grain contact [*McKenzie and McPhedran*, 1977], particle shape [*Jones and Friedman*, 2000] and particle size distribution [*Robinson and Friedman*, 2001].

[19] To extend the comparison with mixing formulas four well-known models were used to test their predictive ability compared with our determined solid permittivity value obtained for hematite ore. The mixing formulas written for the determination of the solid permittivity for a granular mixture in air were; the Lichteneker formula (equation (1a)), the Looyenga formula (equation (2a)) the refractive index model [*Birchack et al.*, 1974]:

$$\varepsilon_s = \left[\frac{\varepsilon_{eff}^{1/2} + F - 1}{f}\right]^2 \tag{9}$$

and the Bruggeman formula, the symmetric effective medium approximation [*Bruggeman*, 1935]:

$$\varepsilon_s = \frac{1 - F - \varepsilon_{eff}^{2/3}}{1 - F - \varepsilon_{eff}^{-1/3}} \tag{10}$$

The percentage error in terms of over and underestimation of the solid permittivity of the hematite ore is given in Figure 6. Equations (1a) and (10) have up to a 20% error, indicating the inadequacy of these models. Equations (2a) and (9) highly underestimate the value of ε_s by 35–40%. This is hardly surprising with equation (9), which describes a physical system of layered dielectrics and not a granular media. This analysis clearly demonstrates the importance of the proposed measuring method for determining the solid permittivity. Values of solid permittivity obtained from a mixing formula must be considered estimates with varying degrees of accuracy.

[20] The range of predictions obtained with the different models highlights some of the difficulties in not having an accurate dielectric mixing model for two-phase granular materials. The method presented in this paper provides the value of ε_s, required to rigorously test proposed dielectric mixing models. Values are also obtained which are valid for the relevant measurement frequency, which is an important consideration with the range of techniques and measurement frequencies used for geophysical measurements.

5.1. Electrical Conductivity of Semiconducting Grains

[21] A further application of the described method is to measure the electrical conductivity of solid grains. Electrical conductivity is widely used in efforts to characterize rock formations [*Archie*, 1942; *Sen et al.*, 1981]. Although the matrix is rarely conducting the method outlined for dielectrics can similarly be applied to determine the electrical conductivity of solid grains, not to be confused with the surface conductivity of adsorbed cations. This is because the dielectric and electrical conductivity problems in two-phase can be treated as analogous [*McKenzie and McPhedran*, 1977].

[22] The results for coarse grained hematite ore and carborundum (SiC) particles are presented in Figures 7a and 7b along with the best fits used to determine the conductivity of the solid. The electrical conductivities determined for the solid were 0.040 dS m^{-1} (r^2 = 0.991) for hematite ore and 10.9 dS m^{-1} (r^2 = 0.998) for the carborundum. The electrical conductivity arises from the structure of the materials and not from adsorbed ions on the surfaces. It is interesting to observe that there is a little more scatter with the hematite data points obtained using electrical conductivity measurements (Figure 7a) than using dielectric measurements. The figures present higher

contrasts, which enhance the effect of grain shape and orientation. The other factor is the contact between grains, the number and area of contact points will allow a certain amount of current to pass between grains rather than the grains act as individual isolators when conductivity of the solid is less than that of the solution. This means that every time the material is repacked with each new solution the number of contact points and their distribution will vary, hence causing a certain amount of scatter in the data. The general method demonstrates a broad applicability for characterizing either dielectric permittivity or the electrical conductivity of the solid matrix of porous granular media.

6. Conclusions

[23] A method of determining the permittivity of granular solids is presented, which relies on the immersion of the solid in a range of dielectric fluids. Results are presented for a number of natural, granular materials including a soil, iron ore, seashell fragments and quartz sand grains. The determined permittivity values demonstrated that estimates of solid permittivity obtained using a dry packing and mixing formula varied in accuracy between 0% and 45%. Eliminating this error with the proposed method should enable dielectric mixing models to be thoroughly tested, as the permittivity of all the phases should be determinable. The Maxwell-Garnett formula best described the data and it might be used to reduce the number of measurements required to determine the permittivity of the solid. The method is extended to apply to the determination of the electrical conductivity of the matrix grains by replacing the immersion dielectric fluids by ionic solutions with a range of electrical conductivities.

[24] **Acknowledgments.** The authors wish to acknowledge the funding provided for this project from the BARD (Project No. IS-2839-97), the United States-Israel Binational Agricultural Research and Development Fund, and the contribution from the Agricultural Research Organization, the Volcani Center, Bet Dagan, Israel, No. 622/00. We are also grateful to Ariel Lazar for carrying out the electrical conductivity measurements and to D. Schmitt, G. C. Topp and S. B. Jones for their helpful comments.

References

Archie, G. E., The electrical resistivity log as an aid in determining some reservoir characteristics, *Trans. AIME*, *146*, 54–62, 1942.

Birchack, J. R., C. G. Gardner, J. E. Hipp, and J. M. Victor, High dielectric constant microwave probes for sensing soil moisture, *Proc. IEEE*, *62*, 93–98, 1974.

Bruggeman, D. A .G., The calculation of various physical constants of heterogeneous substances, 1, The dielectric constants and conductivities of mixtures composed of isotropic substances, *Ann. Phys.*, *24*, 636–664 (in German), 1935.

Carmichael, R. S., *Handbook of Physical Properties of Rocks*, CRC Press, Boca Raton, Fla., 1982.

Chan, C. Y., and R. Knight, Determining water content and saturation from dielectric measurements in layered materials, *Water Resour. Res.*, *35*(1), 85–93, 1999.

Dirksen, C., and S. Dasberg, Improved calibration of time domain reflectometry soil water content measurements, *Soil Sci. Soc. Am. J.*, *57*, 660–667, 1993.

Dobson, M. C., F. T. Ulaby, M. T. Hallikainen, and M. A. El-Rayes, Microwave dielectric behavior of wet soil, 2, Dielectric mixing models, *IEEE Trans. Geosci. Remote Sens.*, *GE-23*(1), 35–46, 1985.

Dube, D. C., Study of Landau–Lifshitz–Looyenga's formula for dielectric correlation between powder and bulk, *J. Phys D. Appl. Phys.*, *3*, 1648–1652, 1970.

Friedman, S. P., A saturation degree-dependent composite spheres model for describing the effective dielectric constant of unsaturated porous media, *Water Resour. Res.*, *34*, 2949–2961, 1998.

Friel, R., and D. Or, Frequency analysis of time-domain reflectometry (TDR) with application to dielectric spectroscopy of soil constituents, *Geophysics*, *64*(3), 1–12, 1998.

Gardner, C. M. K., D. A. Robinson, K. Blyth, and J. D. Cooper, Soil water content measurement, in *Soil and Environmental Analysis: Physical Methods*, 2nd ed., edited by K. Smith and C. Mullins, pp. 25–49, Marcell Dekker, New York, 2000.

Hallikainen, M. T., F. T. Ulaby, M. C. Dobson, M. A. El-Rayes, and L.-K. Wu, Microwave dielectric behavior of wet soil, 1, Empirical models and experimental observations, *IEEE Trans. Geosci. Remote Sens.*, *GE-23*(1), 25–34, 1985.

Heimovaara, T. J., Time domain reflectometry in soil science: Theoretical backgrounds, measurements and models, Ph.D. thesis, Univ. van Amsterdam, Netherlands, 1993.

Heimovaara, T. J., and E. de Water, A computer controlled TDR system for measuring water content and bulk electrical conductivity of soils, *Rep. 41*, Lab. Phys. Geogr. and Soil Sci., Univ. of Amsterdam, Amsterdam, 1993.

Heimovarra, T. J., W. Bouten, and J. M. Verstraten, Frequency domain analysis of time domain reflectometry waveforms, 2, A four component complex dielectric mixing model for soils, *Water Resour. Res.*, *30*(2), 201–209, 1994.

Jones, S. B., and S. P. Friedman, Particle shape effects on the effective permittivity of anisotropic or isotropic media consisting of aligned or randomly oriented ellipsoidal particles, *Water Resour. Res.*, *36*, 2821–2833, 2000.

Kraszewski, A. W., (Ed.), *Microwave Aquametry Electromagnetic Wave Interaction With Water-Containing Materials*, IEEE Press, Piscataway, N. J., 1996.

Lichtenecker, K., Die dielektrizitatskonstante naturlicher und kunstlicher mischkorper, *Phys. Z.*, *27*, 115–158, 1926.

Lide, D., *Handbook of Physics and Chemistry*, CRC Press, Boca Raton, Fla., 1999.

Looyenga, H., Dielectric constants of mixtures, *Physica*, *31*, 401–406, 1965.

Lord Rayleigh, On the influence of obstacles arranged in rectangular order upon the properties of the medium, *Philos. Mag.*, *34*, 481–502, 1892.

Maxwell-Garnett, J. C., Colours in metal glasses and in metallic films, *Philos. Trans. R. Soc. London, Ser. A.*, *203*, 385–420, 1904.

McKenzie, D. R., and R. C. McPhedran, Exact modelling of cubic lattice permittivity and conductivity, *Nature*, *265*, 128–129, 1977.

Nelson, S. O., Estimation of permittivities of solids from measurements of pulverized or granular materials, in *Dielectric Properties of Heterogeneous Materials*, PIER 6. Prog. Electromagn. Res., edited by A. Priou, pp. 231–271, Elsevier Sci., New York, 1992.

Nelson, S. O., and T-S. You, Relationships between microwave permittivities of solid and pulverized plastics, *J. Phys D. Appl. Phys.*, *23*, 346–353, 1990.

Nelson, S. O., D. P. Lindroth, and R. L. Blake, Dielectric properties of selected minerals at 1–22 GHz, *Geophysics*, *54*(10), 1344–1349, 1989.

Olhoeft, G. R., Electrical properties of rocks, in *Physical Properties of Rocks and Minerals*, *McGraw-Hill/CINDAS Data Series on Material Properties*, vol. II-2, edited by Y. S. Touloukian and C. Y. Ho, pp. 298–329, McGraw-Hill, New York, 1981.

Robinson, D. A., and S. P. Friedman, The effect of particle size distribution on the effective dielectric permittivity of saturated granular media, *Water Resour. Res.*, *37*, 33–40, 2001.

Sen, P. N., C. Scala, and M. H. Cohen, A self-similar model for sedimentary rocks with application to the dielectric constant of fused glass beads, *Geophysics*, *46*(5), 781–795, 1981.

Sihvola, A., Dielectric mixture theories in permittivity prediction: Effect of water on macroscopic parameters, in *Microwave Aquametry Electromagnetic Wave Interaction With Water-Containing Materials*, edited by A. W. Kraszewski, IEEE Press, Piscataway, N. J., 1996.

Sihvola, A., and J. A. Kong, Effective permittivity of dielectric mixtures, *IEEE Trans. Geosci. Remote Sens.*, *26*(4), 420–429, 1988.

Topp, G. C., J. L. Davis, and A. P. Annan, Electromagnetic determination of soil water content: Measurements in coaxial transmission lines, *Water Resour. Res.*, *16*, 574–582, 1980.

von Hippel, A. R., (Ed.), *Dielectrics Materials and Applications*, MIT Press, Cambridge, Mass., 1954.

S. P. Friedman, Institute of Soil, Water, and Environmental Sciences, ARO, Volcani Center, Bet Dagan, Israel.

D. A. Robinson, US Salinity Laboratory, USDA, 450 West Big Springs Road, Riverside, CA 92507, USA. (drobinson@ussl.ars.usda.gov)